Plant Soil
https://doi.org/10.1007/s11104-023-06146-9

RESEARCH ARTICLE

# A novel method for in situ imaging of root exudates and labile elements reveals phosphorus deficiency-induced mobilization of rare earth elements in the rhizosphere of *Phytolacca americana*

**Chong Liu · Ting-Xuan Ding · Antony van der Ent · Chang Liu · Jean Louis Morel · Catherine Sirguey · Wen-Shen Liu · Ye-Tao Tang · Rong-Liang Qiu**

Received: 23 February 2023 / Accepted: 26 June 2023


**Abstract**

*Aims* Phosphorus (P) deficiency-induced mobilization of rare earth elements (REEs) in the rhizosphere contributes to REE accumulation in the hyperaccumulator *Phytolacca americana*, but a lack of in situ methods for visualization of the root-soil interface limits our understanding of the underlying processes.

*Methods* Diffusive gradients in thin-films (DGT) devices were used for probing root exudates, REEs and P in the *P. americana* rhizosphere. Desorption electrospray ionization mass spectrometry and laser-ablation inductively coupled mass spectrometry were used for in situ imaging of root exudates, REEs and P sorbed on the DGT.

*Results* The novel approach demonstrated here is capable of synchronously and quantitatively characterizing the distribution of root exudates and labile elements in the rhizosphere. The secretion fluxes of citrate and oxalate in the rhizosphere under P deficiency were three times higher than under P sufficient condition; and the lanthanum (La) fluxes in the rhizosphere under P deficiency were ten times greater than at P sufficiency condition. The enrichment of P and La under P deficiency and depletion under P sufficient conditions in the rhizosphere suggests that P deficiency-induced organic acid secretion is crucial

Responsible Editor: Juan Barcelo.

**Supplementary information** The online version contains supplementary material available at https://doi.org/10.1007/s11104-023-06146-9.

C. Liu · T.-X. Ding · C. Liu · W.-S. Liu (✉) · Y.-T. Tang · R.-L. Qiu
School of Environmental Science and Engineering, Sun Yat-sen University, Guangzhou 510006, China
e-mail: liuwsh8@mail.sysu.edu.cn

C. Liu
Institute of Agricultural Resources and Environment, Guangdong Academy of Agricultural Sciences, Guangzhou 510640, China

A. van der Ent
Laboratory of Genetics, Wageningen University and Research, Wageningen 6708 PB, The Netherlands

A. van der Ent · J. L. Morel · C. Sirguey
Laboratoire Sols et Environnement, INRAE, Université de Lorraine, Nancy 54000, France

A. van der Ent
Centre for Mined Land Rehabilitation, Sustainable Minerals Institute, The University of Queensland, Brisbane, QLD 4072, Australia

W.-S. Liu · Y.-T. Tang
Guangdong Provincial Key Laboratory of Environmental Pollution Control and Remediation Technology, Guangdong Provincial Engineering Research Center for Heavy Metal Contaminated Soil Remediation, Sun Yat-sen University, Guangzhou 510006, China

R.-L. Qiu
Guangdong Laboratory for Lingnan Modern Agriculture, Guangdong Provincial Key Laboratory of Agricultural & Rural Pollution Abatement and Environmental Safety, College of Natural Resources and Environment, South China Agricultural University, Guangzhou 510642, China

Published online: 14 July 2023

for the mobilization of soil REEs and subsequent REE accumulation in *P. americana*.

*Conclusion* The combination of DGT devices with mass spectrometry imaging is technically feasible for in situ synchronous imaging of root exudates, REEs and labile elements at the root-soil interface. Our study shed light on processes of mobilization of mineral elements in the rhizosphere induced as a side-effect of the P acquisition mechanism.

**Keywords** Root exudates · Mass spectrometry imaging · Rhizosphere effect · Spatial distribution · DGT

## Introduction

Hyperaccumulators are plants that accumulate metal(loid)s in their leaves exceeding nominal element threshold criteria whilst successfully completing their life cycle (van der Ent et al. 2013). The (hyper)accumulation of some metals or metalloids in a number of hyperaccumulator species is, to a large extent, a side-effect of nutrient acquirement (i.e., inadvertent uptake) (Pollard 2022; Pollard et al. 2014). This includes phosphorus (P) deficiency-induced rhizosphere acidification inadvertently causing mobilization of soil manganese (Mn) leading to Mn hyperaccumulation in *Phytolacca americana* (DeGroote et al. 2018). The P acquisition strategy also facilitates rare earth element (REE; the lanthanides and yttrium) mobilization in the soil by ligand complexation and $H^+$ competition, leading to inadvertent REE accumulation in some plants species (e.g., lupin) (Monei et al. 2022; van der Ent et al. 2022; Wiche et al. 2016). In previous studies, we have shown that P deficient conditions induce an increased secretion of protons and organic acids in the rhizosphere *P. americana*, and this process not only promotes the mobilization of soil P, but also causes the release of REEs in the soil and subsequent uptake of REEs (Liu et al. 2021, 2023). However, it remains unclear how plant root exudates and soil P in the rhizosphere interact with each other to affect REE availability.

The rhizosphere refers to the small volume of soil that surrounds living roots and is of great importance to the mobilization and bioavailability of plant nutrients and other trace elements (Badri and Vivanco 2009). Plant root exudates, especially organic acids, are one of the major driving forces for solubilization of mineral nutrients in the rhizosphere soils and the subsequent root uptake (Chen et al. 2017; Singh et al. 2016; Tao et al. 2016; Tiziani et al. 2022). A range of simple, but useful methods, such as exogenous addition of organic acids and artificial separation of bulk and rhizosphere soils, have been used for studying the physio-chemical changes induced by root exudates (Tao et al. 2020; Yang et al. 2021). However, these methods are usually not sensitive enough to detect rhizosphere effect, due to the very small volume of rhizosphere soil (Kuzyakov and Razavi 2019; Oburger and Jones 2018). Therefore, in order to quantitively observe rhizosphere processes and root exudate-mineral element interactions at the root-soil interface, it is imperative to develop methods for in situ determination of the root exudates and mineral elements (Kuzyakov and Razavi 2019).

Visualization of 2D and 3D rhizosphere processes *via* chemical and non-invasive imaging has significantly enhanced our knowledge of rhizosphere processes across a range of scales from cm to sub-mm (Gregory et al. 2022; Oburger and Schmidt 2016). One of these methods, diffusive gradients in thin films (DGT), has been intensively used to characterize the distribution of elements in soils and measure the bioavailability of a variety of anions and cations (Guan et al. 2021). The DGT method has been widely used in rhizosphere visualization due to its advantages of in situ measurement and high spatial resolution (~ 100 μm) (Álvarez-López et al. 2021; Davison and Zhang 1994; Williams et al. 2014). Other methods have also been used for quantification of root exudates, including hydroponic culture-based approaches and soil-based approaches (e.g., the "quick and dirty" root washing) (Oburger and Jones 2018). However, most of these existing methods for collection of root exudates are destructive, and thus cannot provide accurate in situ spatial distribution of the target analytes (White et al. 2017). Moreover, thus far no attempts have been made to in situ visualization of root exudates and mineral elements simultaneously.

Mass spectrometry imaging (MSI), a molecular imaging technology which combined with mass spectrometry and imaging technology, can directly provide information on the spatial distribution of biomolecules. MSI is mostly used in the field of biomedicine (Bhandari et al. 2015), but has rarely been employed to explore the root exudate mediated processes. Using a hydrophobic polyvinylidene fluoride (PVDF) membrane and matrix assisted laser desorption ionization

mass spectrometry (MALDI-MS), Veličković et al. (2020) localized the spatial distribution of some metabolites in switchgrass rhizosphere. However, this method was not able to provide information on the spatial distribution of organic acids. Tiziani et al. (2021) used DGT devices with zirconium hydroxide binding layer (-ZrOH) to characterize the spatial in situ distribution of citrate in white lupin root exudates, but the complexity of operation and relatively low resolution means that it has limited application. A recent study showed that MALDI-MS can be used to obtain information on the spatial distribution of lysimachic acid secretion under P deficient conditions (Gomez-Zepeda et al. 2021). However, this study was based on an artificial medium rather than natural soil. In conclusion, approaches for in situ quantitative visualization of the spatial distribution of root exudates are still lacking, and there has been no attempt yet to combine MSI with DGT to link root exudates and metal dynamics in the rhizosphere.

Therefore, the aims of this study were: (i) to develop an approach for in situ simultaneous imaging of root exudates and elements in the rhizosphere; (ii) to reveal the spatial distribution of REEs, P and root exudates in the rhizosphere of *P. americana*; (iii) to clarify the interaction process of REEs, P and root exudates in the rhizosphere hotspots. The combination of the above sub millimeter imaging technologies is expected to achieve a clear picture of P deficiency-induced mobilization of REEs in the rhizosphere of *P. americana*.

## Materials and methods

### Rhizobox experiment and experimental rhizosphere for imaging

The soils material for the experiments was collected from REE mine tailings (115.032291°E, 24.99591°N) near Ganzhou city, Jiangxi province, China. The soils had low organic matter content and was nutrient deficient (e.g., N and P), but has high REE concentrations ($435 \pm 30.6$ mg $kg^{-1}$, Table S1). Due to the barren properties of soils, approximately 1% (dry weight) biochar was added to the soil (2 mm) to support plant growth. This proportion of biochar addition has limited stabilization effect on REEs (Liu et al. 2020). The biochar was made from sawdust that was anaerobically carbonized at 500℃ for 1 h. The chemical analysis and physicochemical properties of the soil and biochar are shown in SI Materials and Methods and Table S1.

The amended soils were used to fill rhizoboxes ($14 \times 4 \times 21$ cm) with a detachable side. The rhizoboxes filled with soils were watered with ultrapure water to reach 65% field capacity by weight and the rhizoboxes were homogenized for three weeks. The germinated seeds of *P. americana* were sown into these soil-filled rhizoboxes, which were then wrapped with aluminum foil and kept inclined at 45° to promote root growth onto the detachable side. This process created an experimental rhizosphere for subsequent imaging. The rhizoboxes were places in a climate chamber with the growth condition as follows: day 25℃/night 20℃, humidity 60–70%, illumination time 16 h, intensity 250–300 μmol $m^{-2}$ $s^{-1}$. During the experiment, the soil water content was maintained at 65% of field capacity by weighing every 4 days.

### Mass spectrometry imaging of root exudates in rhizosphere by desorption electrospray ionization mass spectrometry (DESI-MS)

#### *In situ sampling of root exudates*

A hydrophilic PVDF membrane was used to imprint organic acids from experimental rhizosphere. This is because the compatibility of the surface chemistry of this membrane with the negative ionization mode required for organic acid detection (Veličković et al. 2020). The PVDF membrane (Durapore® PVDF, Millipore) has a pore size of 0.45 μm, a diameter of 47 mm and a thickness of 100 μm. After four weeks of cultivation of the plants, the regions of interest (ROIs) on the detachable side of rhizoboxes were selected according to their root growth (Fig. 1a). The root system was imaged with a digital camera after removing the side plate and the PVDF imprinting membrane was subsequently placed on the ROI (Fig. 1b), and the side plate was re-installed again. During the process of membrane adsorption, any moving of membrane and detachable side of rhizoboxes was strictly avoided. After 24 h, the side plate was carefully removed and the PVDF membrane was recycled. To reduce contamination from soil particles, the soil particles adhered to the PVDF

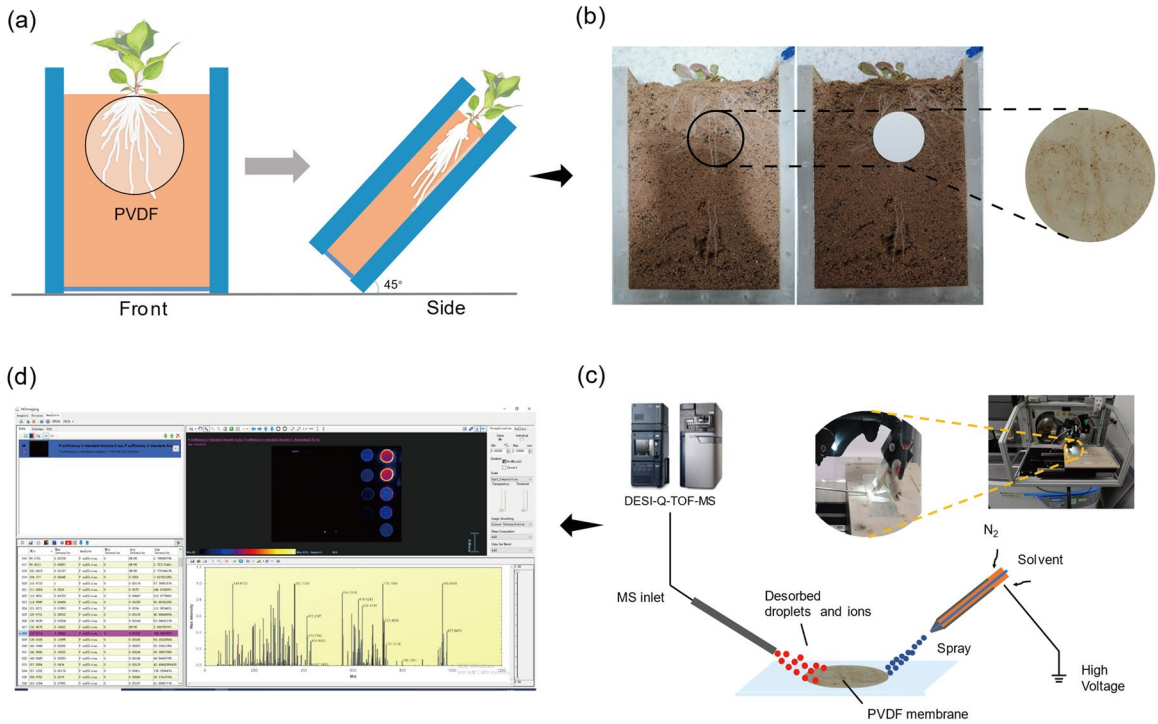


**Fig. 1** The workflow for DESI-MS imaging of root exudate of organic acids in rhizosphere of *P. americana*. **a** *P. americana* planted in rhizoboxes with a detachable side. **b** The PVDF membrane was installed on the root-soil interface and developed for 24 h; **c** The PVDF imprinting membrane was mounted on the sample stage to be subjected to DESI analysis. **d** The obtained raw data from DESI-MS were imported into HDImaging v1.4 software for further processing. DESI-Q-TOF-MS, desorption electrospray ionization - quadrupole-time of flight- mass spectrometry

membrane were removed by forced air using an aurilave. The deployed imprinting membrane was then affixed onto Omni Slide MT-96 (Prosolia lnc., USA) with double-sided tape. The slides were immediately mounted onto the sample stage for the DESI analysis (Waters, USA) (Fig. 1c).

*DESI imaging of root exudates*

DESI-MS refers to the method using charged solvent droplets to desorb and ionize species from the sample for mass spectrometry analysis. Combined with imaging software, the spatial distribution of target molecule are in situ imaged (Veličković and Anderton 2017). The photograph of the slides with the PVDF membranes were loaded into HDImaging v1.4 (HDI) software (Waters, USA). The detail DESI parameters are shown in SI Materials and Methods. The obtained raw data from DESI-MS were imported into HDI for data processing (Fig. 1d). The processing parameters were set as follows: the number of most intense peaks 1000, whole mass range, enable lock mass at 554.2620 m/z.

*DESI imaging of standard organic acids*

In order to quantify the adsorption of organic acids on the PVDF membrane, calibration was performed by adding organic acids on PVDF membrane as follows. Three types of organic acids (i.e., citrate, malate, and oxalate) (Sigma-Aldrich, USA) were used to prepare the calibration solutions. One microliter mixed organic acid solutions with different concentrations (0, 0.1, 0.25, 0.5, 1.0, 2.5, 5.0, 10, 25, 50 mmol $L^{-1}$) were slowly added dropwise onto the PVDF membrane. After that, the PVDF membrane was affixed onto the glass slide with double-sided tape. The slide was immediately mounted on the sample stage to conduct the DESI-MS analysis after acquiring an image with a fixed distance between the camera and

the slide. The circular area of each calibration point of organic acids was selected with the ROI tool in HDI to obtain average intensity values. The intensities and corresponding concentrations of organic acid were subjected to linear fitting using Origin software (Pro 2021b, OriginLab Corporation, USA).

## Synchronous imaging of the spatial distribution of root exudates and elements in *P. americana* rhizosphere

### *Rhizobox experiment with distinct P treatments*

In order to investigate the relationships between REEs, P and root exudates in the rhizospheres, another rhizobox experiment was conducted. In this experiment, the P supply, 0 mmol $L^{-1}$ ("−P") and 2 mmol $L^{-1}$ ("+P") $KH_2PO_4$ (dry weight) were amended into the tailing soil material, respectively. Then 160 mL of Hoagland solution (pH 5.3, Table S2) was added to all the treatments to support plant growth. The soil solution was collected once a week with a porewater sampler (Rhizon MOM, 19.21.21f, Netherlands) following the methods described in Liu et al. (2020). The collected soil solutions were immediately frozen at − 80 ℃ until analysis.

### *Synchronous imaging of root exudates and elements by DESI-MS and laser-ablation inductively coupled mass spectrometry (LA-ICP-MS)*

Diffusive gradients in thin-films (DGT) are a passive sampler composed of binding gel, diffusion gel and filter membrane. By simulating the migration of elements to the root surface through DGT, the concentrations of bioavailable chemicals in soil are in situ detected (Guan et al. 2021). DGT devices were used to reveal the spatial distribution of root exudates, REEs and P. The DGT device was composed of a PVDF filter membrane (0.45 μm, Durapore®, Millipore, USA; for root exudates), binding gel (0.40 mm, Chelex-100 resin, zirconium hydroxide precipitate; for REEs, P, etc.) and diffusion gel (0.80 mm, 1.5% agarose) (Nanjing Easysensor Environmental Technology Co., Ltd., China). The preparation and installation of these flat-panel high-resolution DGT devices followed the methods described in Ren et al. (2021). After 4 weeks of plant growth, the region of interest (ROI) on the removable side of the rhizobox was selected and DGT device was installed. During the DGT deployment, the PVDF membrane was close to the root-soil interface, and the binding gel and the diffusion gel were attached onto the PVDF membrane respectively (Fig. 2).

After 24 h-deployment, the rhizobox side was removed, and the PVDF membrane was recycled. The soil particles adhered to the PVDF membrane were removed by forced air using aurilave. The PVDF membrane was affixed onto the slide (Omni Slide MT-96, Prosolia lnc., USA) with double-sided adhesive tape. To identify organic acids in the membrane, 1 μL organic acid standard solution (1 μmol $L^{-1}$) was slowly added on another small piece of PVDF membrane, and then immediately stick the small piece of membrane next to the sample on the slide. The slide was immediately mounted on the sample stage for the DESI-MS analysis (Fig. 1b). The left DGT device (binding gel and diffusion gel) was retrieved and rinsed with a jet of ultrapure water. The binding gels were dried (50℃, 3 h) using a vacuum gel dryer (GDS2000D, Life Technologies, USA). The dried gels were then subjected to the LA-ICP-MS analysis.

LA-ICP-MS use high-energy laser beam to focus on the sample surface, where the particles generated by ablation are transported to ICP-MS and subsequently introduced into the mass spectrometer detector (Günther and Hattendorf 2005). LA-ICP-MS was used to visualize the spatial distribution of labile elements bound in binding gel of DGT. To quantitatively analyze the elements bound in binding gel using LA-ICP-MS, calibration standards for LA-ICP-MS were prepared by immersing the HR-ZCA binding gel assembled in the DGT samplers (3.14 cm in diameter) into solutions containing different concentrations of REEs, P and mineral elements (Mn, Zn, etc.) (4 replicates). After 24 h of immersion, three replicate of binding gels were used for acid digestion and determination of the total amount of target elements by ICP-MS. The other one replicate of binding gel was dried and then analyzed by LA-ICP-MS with sample and sample blank. The samples were collected using a laser ablation system (NWR imagegeo193, elemental scientific, USA), and ionic signal intensity was obtained by ICP-MS (icpTOF R, Tofwerk, Switzerland). To improve the analysis accuracy, internal standard correction was carried out according to the method of Lehto et al.

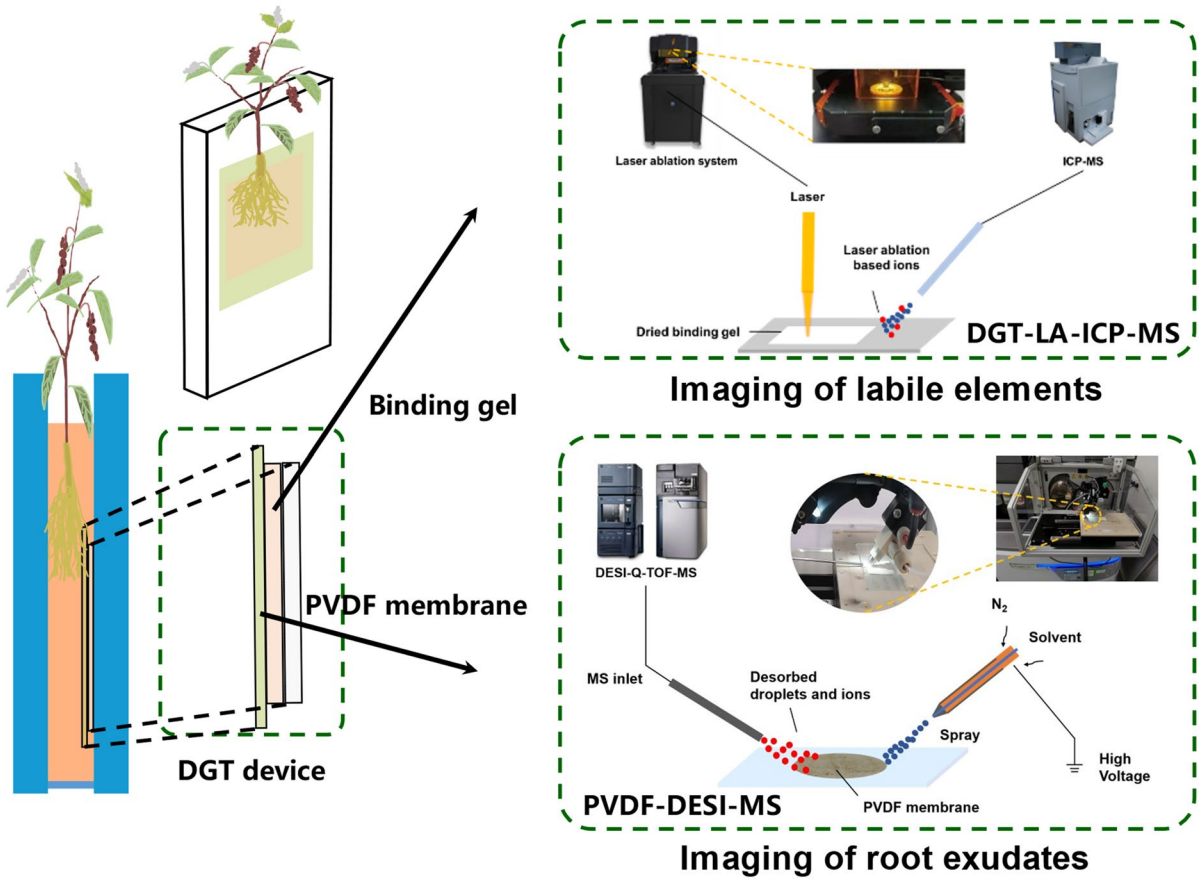


**Fig. 2** The workflow for the imaging of root exudate of organic acids and labile elements in the rhizosphere of *P. americana*. The polyvinylidene fluoride (PVDF) membrane, binding gel, and diffusion gel were installed on the root-soil interface and saturated for 24 h (left); The PVDF imprinting membrane and the binding gel of diffusive thin gradients in thin-films (DGT) were subjected to desorption electrospray ionization mass spectrometry (DESI-MS) and laser ablation inductively coupled plasma mass spectrometry (LA-ICP-MS) analysis, respectively (right)

(2012). Since $^{13}$C is the main element of the binding gel matrix, $^{13}$C is used as the internal standard for standardization (Ren et al. 2021). The parameters for the analysis of LA-ICP-MS are provided in SI Materials and Methods.

After the demounting of the DGT devices, the plants were harvested and separated into roots and shoots and carefully rinsed with ultrapure water. Root samples were soaked in 5 mM $CaCl_2$ for 15 min (4℃) for desorption of ions (Han et al. 2005). The dry weight of plant samples was recorded after drying at 65℃ for 72 h. The plant samples were then ground with a mortar and sieved to ≤ 1 mm. The plant powder was subsequently digested with $HNO_3$:$H_2O_2$ (3: 1) at 190℃ for 30 min using a microwave digestion system (MARS6, CEM, USA). The determination of P and metal concentrations in the plant samples was the same as described above.

*Image processing and analysis*

Root-soil interface photographs, root exudate imaging maps, and elemental imaging maps were captured or generated by cameras, DESI-MS, and LA-ICP-MS, respectively. For root exudate imaging maps, the obtained raw data from DESI-MS were imported into the HDI software for processing. The image parameter inputs were the same as described above. The mass to charge ratio (m/z), intensity and the coordinate profiles of the corresponding compounds were obtained in the HDI software. The regions of interest (ROI) were selected by using the HDI ROI tool, and

then the extracted MS information from all ROIs were exported by MVA for multi-variate analysis (Fig. 1d). The elemental imaging maps were generated by Surfer software. Root-soil interface photographs, imprinting membrane images, root exudate imaging maps, and elemental imaging maps were aligned using Adobe Illustrator (CC 2019, Adobe Systems Incorporated).

### Statistical analysis

The intensity values of organic acids in each coordinate were converted into concentrations using the calibration curve, and the spatial distribution of organic acids was obtained by Origin (Pro 2021b, OriginLab Corporation, USA). The linear fit was performed by Origin (Pro 2021b, OriginLab Corporation, USA). Student's t-test was employed to compare the difference of plant biomass and element concentration between P sufficiency and P deficiency treatments.

## Results

### Plant growth and element accumulation

The root and leaf dry weights of *P. americana* under P deficient conditions were 0.60±0.21 g, were significantly lower than those of plants grown on P amended soil (1.46±0.12 g, 1.13±0.12 g) (Fig. 3a). The REE concentration in the leaf of *P. americana* under P deficient conditions were 832±56.2 mg $kg^{-1}$, which was 1.4-times higher than those of plants grown on P sufficient soil (591±87.1 mg $kg^{-1}$) (Fig. 3b). For nutrient accumulation, P and Mn concentrations in organs of *P. americana* grown in P sufficiency were 1.5–3.0 times higher than those in the P deficient treatments. However, plants under P deficient conditions had 1.1–1.6 times higher Fe, Ca and Mg concentrations in root and stem than plants under P sufficiency (Table S2).

### Effects of P supply on soil solution chemistry

The pH values of *P. americana* rhizosphere soil solutions were about the same at the first week, while the pH of both treatments increased with plant growth. The P deficient treatment had a lower pH value (0.3 pH units) of soil solution than that of P sufficiency in the fourth week (Fig. 4a). However, the REE concentration in soil solution decreased with plant growth, and in the P deficient treatment had 1.6 times higher REE concentration than that of P sufficient conditions in the fourth week (Fig. 4b). There were no significant differences in TOC and P concentrations between P deficient and P sufficient treatment groups (Fig. 4c and d).

### Validation of root exudates imprinted on the PVDF by DESI-MS

In order to validate the root exudates imprinted on the PVDF, the relationship between the masses of

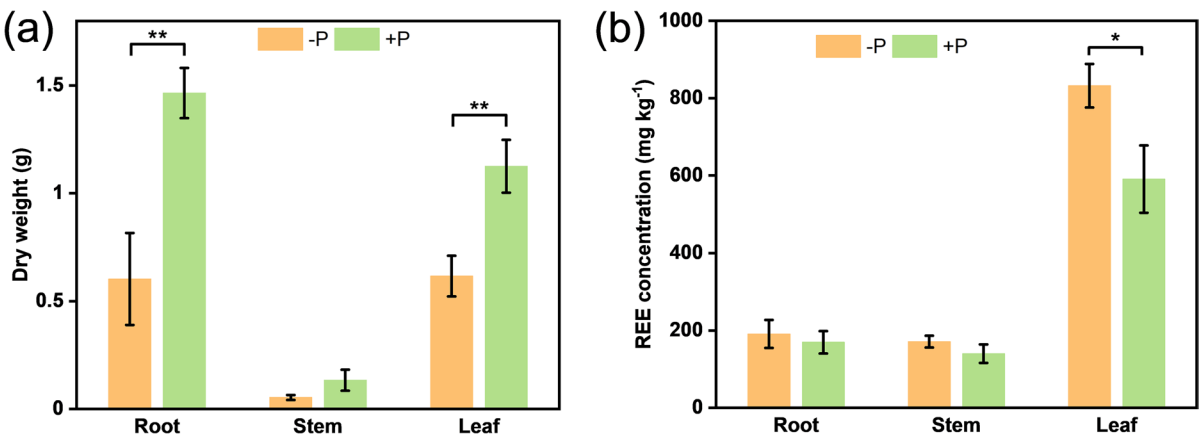


**Fig. 3** Plant growth (**a**) and REE accumulation (**b**) of *P. americana* under different phosphorus (P) treatments. −P, P deficient; +P, P sufficient conditions. Significant differences between P deficient and P sufficient treatments are indicated by asterisks (*, $p<0.05$, **, $p<0.01$, Student's test, $n=3$)

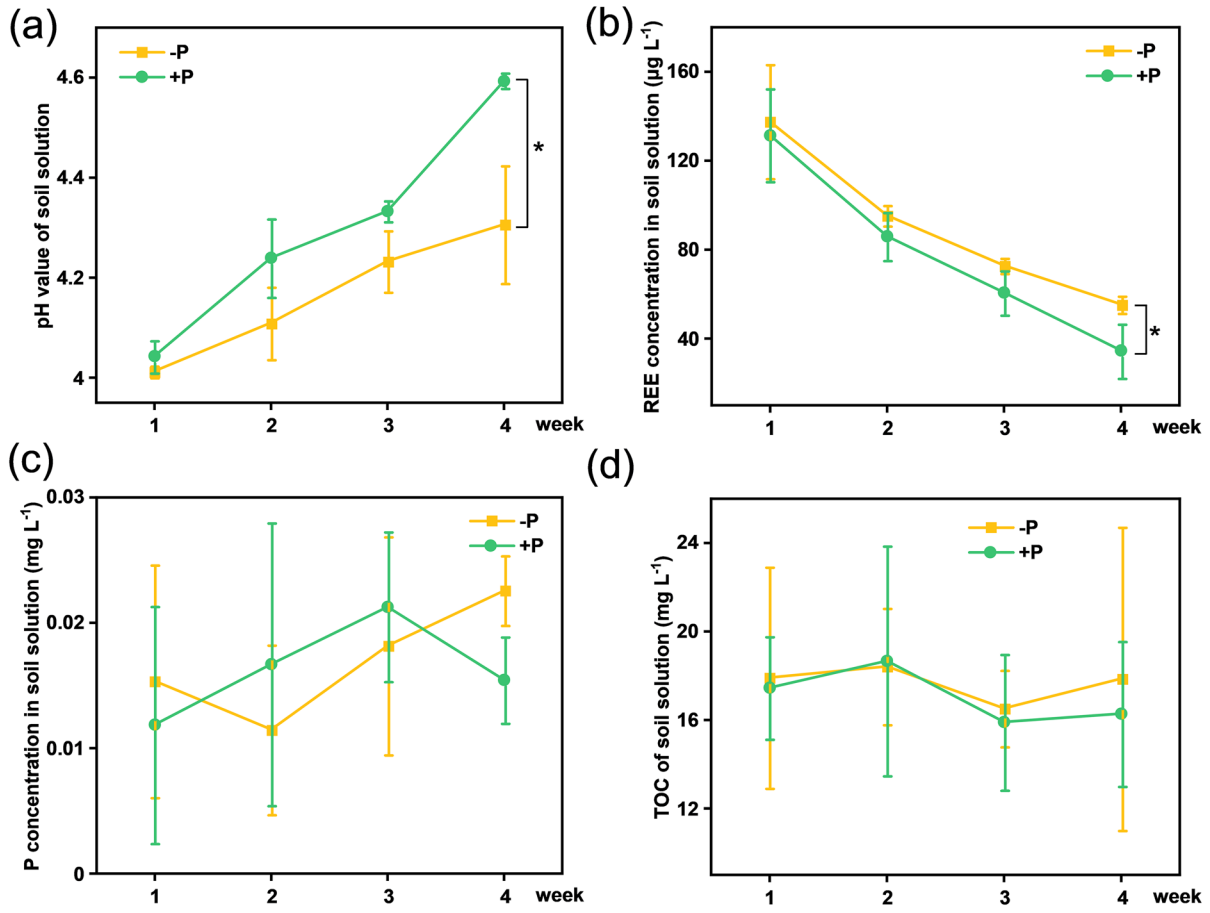


**Fig. 4** Dynamics of pH (**a**), REE (**b**), P (**c**) and **d** total organic carbon (TOC) concentrations in the soil solution in *P. americana*. −P, P deficient; +P, P sufficient conditions. Significant differences between P deficient and P sufficient conditions are indicated by asterisks (*, $p < 0.05$, Student's test, $n = 3$)

standard organic acids accumulated on PVDF and intensity measured by DESI-MS was examined. As the concentrations of standard organic acids increased, the brightness of the circular area containing the standard solution gradually increased (Fig. 5a). Moreover, linear correlations were observed between the accumulated mass of organic acids (i.e., citrate, malate, and oxalate) on PVDF membrane and the corresponding DESI intensity values ($R^2 > 0.95$, Fig. 5b, c, d).

Figure 6 shows the root system and the root exudate maps of *P. americana* generated by DESI with a resolution of 300 × 300 µm. The zone of root exudates was strongly co-localized with the root zone, particularly in the area with dense root formation. Two spatially distinct areas were found in PVDF imprinting membrane of the rhizobox from the DESI analysis. Organic acids constituted the first area, which located in three dense root areas. Among the detected organic acids, oxalate was the most abundant followed by malate and citrate. The second area comprised of high-molecular weight root exudates, such as m/z 539.1583, m/z 709.3835 and m/z 761.3458, which co-localized with the entire root zone especially axial root (Fig. 6, Fig. S1).

## The distribution of REEs, P and root exudates in rhizosphere

To explore the interaction between REEs, P and root exudates in the rhizosphere of *P. americana*, the

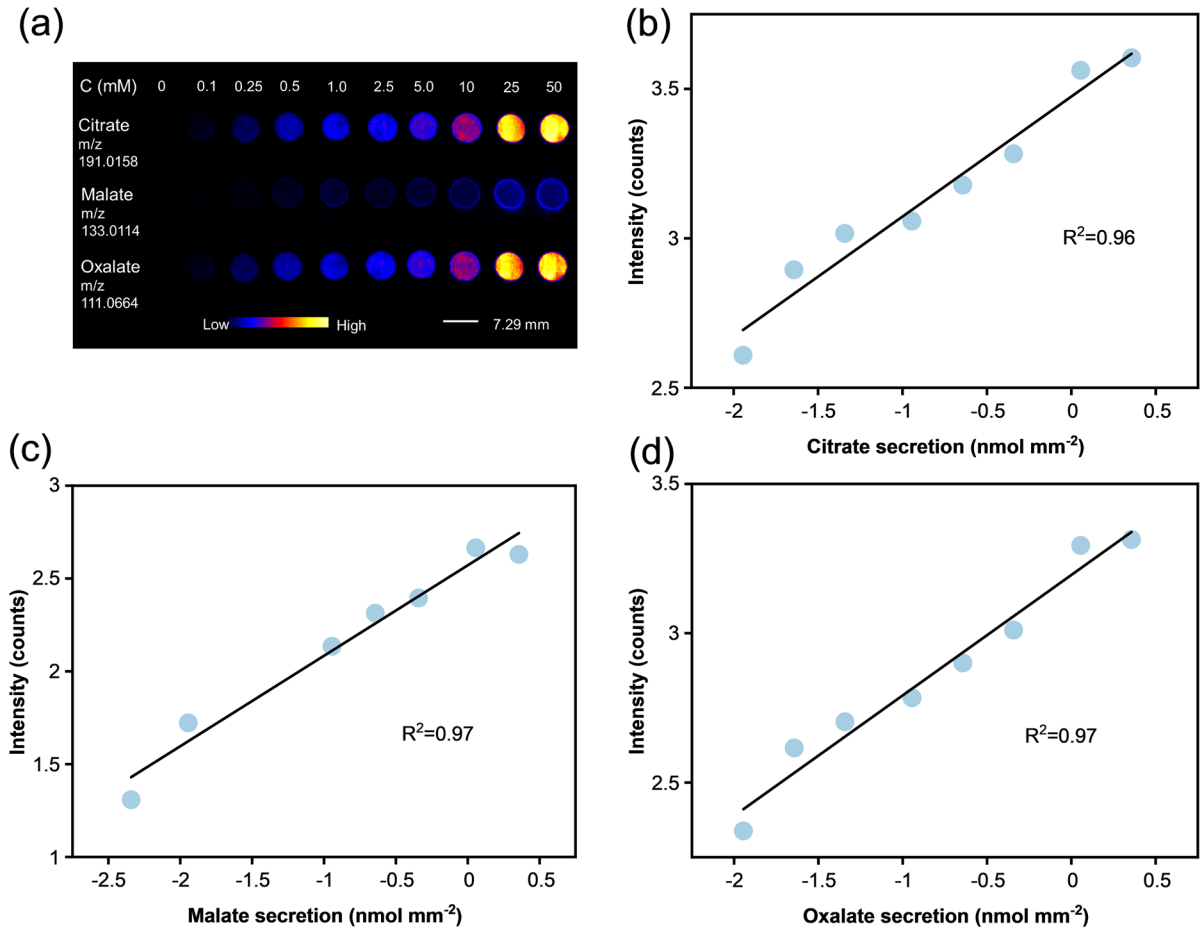


**Fig. 5** Linear correlations between the intensities of the calibration membranes and the organic acids calculated from the concentration of calibration solutions added on the PVDF imprinting membrane. **a** brightness of circle area containing the standard solution; **b-d** correlations between the accumulated mass of organic acids on the PVDF membrane and the corresponding DESI intensity. All data were log-transformed before further analysis. The circle areas of the standard solutions were 22 $mm^2$

spatial distribution of lanthanum (La), P and organic acids secreted by roots under different P treatments were studied by LA-ICP-MS and DESI-MS. It can be seen from Fig. 7 that in the coupling of DESI and LA-ICP-MS, the spatial distribution of root exudates and labile elements was not ideal. Due to the partial diffusion, the spatial distribution of organic acids, La and P at the soil-root interface can be hardly distinguished. However, differences can be found in the rhizosphere of +P and -P treatments. The citrate and oxalate fluxes in the rhizosphere of *P. americana* under P deficiency were the highest, about $2\times10^{-6}$ pmol $mm^{-2}$ $h^{-1}$ and $4\times10^{-5}$ pmol $mm^{-2}$ $h^{-1}$ respectively; while those under P sufficiency treatment was about $0.6\times10^{-6}$ pmol $mm^{-2}$ $h^{-1}$ and $1.2\times10^{-5}$ pmol $mm^{-2}$ $h^{-1}$ respectively, which was only one third of the P deficiency treatment. The P and La fluxes in the rhizosphere were the highest under P deficient conditions, which were 1.0 μg $cm^{-2}$ $s^{-1}$ and 10 μg $cm^{-2}$ $s^{-1}$ respectively (Fig. 7). However, the P and La fluxes in the rhizosphere were the lowest in the P sufficient treatment (1.5 μg $cm^{-2}$ $s^{-1}$ and 1.0 μg $cm^{-2}$ $s^{-1}$ respectively). Compared with the P sufficient treatment, the P, La and mineral elements (e.g., Cu, Mn and Mo) in the rhizosphere of *P. americana* in the P deficient treatment all showed obvious mobilization effects (Fig. 7, Fig. S2).

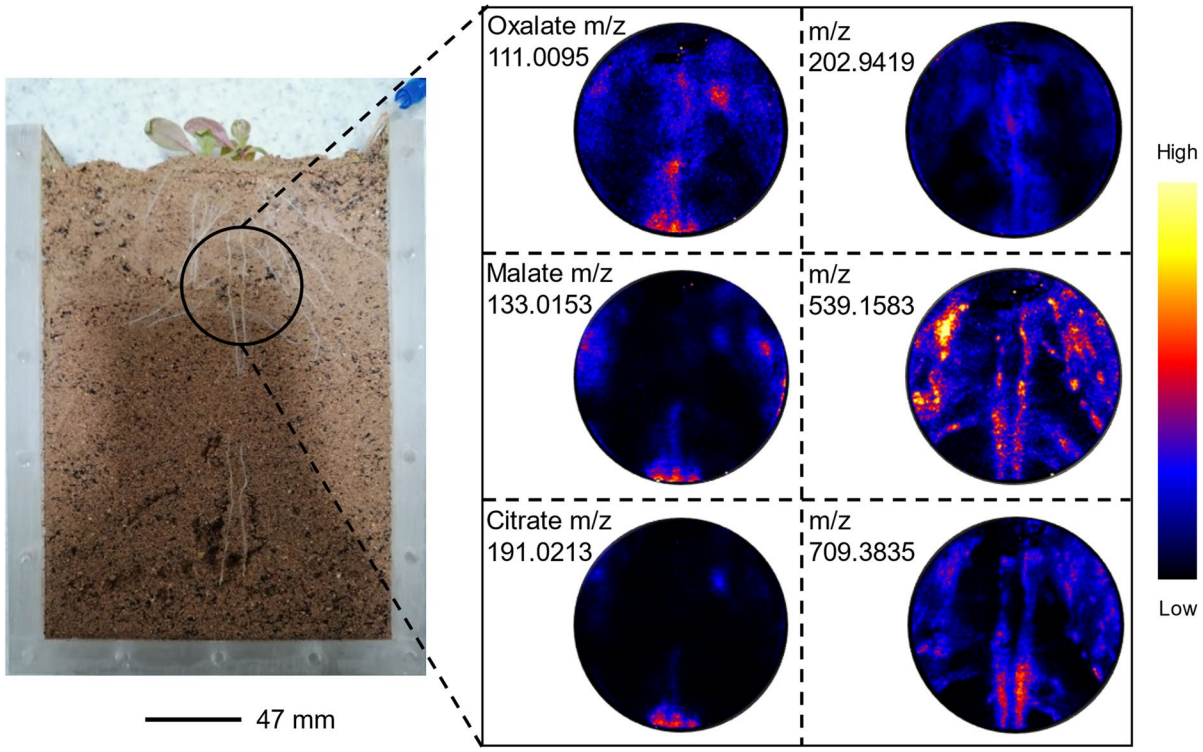


**Fig. 6** DESI-MS imaging of root exudates in the rhizosphere of *P. americana*. (left) The root system of *P. americana* and the selection of regions of interest (black circle). (right) The spatial distribution of organic acids and other metabolites in rhizosphere

## Discussion

### Application of combined imaging in visualization of rhizosphere process

The imaging methods of root exudates reported in previous studies have increased our understanding of rhizosphere effects. However, there are also shortcomings that remain to be solved, such as destructive sampling, their complex operation, non-quantitative imaging, and limited access to small molecular organic acids of root exudates. In this study, the hydrophilic PVDF membrane and DESI-MS analysis were combined to quantitatively obtain the in situ imaging of root exudates in root-soil interface of *P. americana*. The hydrophilic PVDF membrane is suitable for the imaging of low molecular organic acids in the rhizosphere (Fig. 5) because of the compatibility of surface chemistry of the PVDF membrane with negative ionization mode analysis of DESI-MS (Veličković et al. 2020). Under the conditions of this study, the spatial distribution resolution of *P. americana* root exudates can reach 50 μm (Fig. 6), which is much higher than in previous studies (Tiziani et al. 2021). In addition, matrix interferences can be avoided and the target analyte can be expanded to include multiple molecules from low to high molecular weight. Therefore, the PVDF membrane sampling combined with DESI-MS analysis had important advantages in quantifying the in situ distribution of root exudates, including its simple operation, high resolution and low interference.

To our knowledge, there are no reports on synchronously and quantitatively imaging of root exudates and labile elements in situ. In this study, we for the first time show the combination of PVDF-DGT sampling with LA-ICP-MS and DESI-MS imaging analysis, indicating that the coupling of DGT and DESI imaging analysis is technically feasible, and can synchronously and quantitatively provide information on the spatial distribution of labile elements and root exudates in the rhizosphere with sub millimeter resolution. The two sampling methods noted above are non-destructive, and can

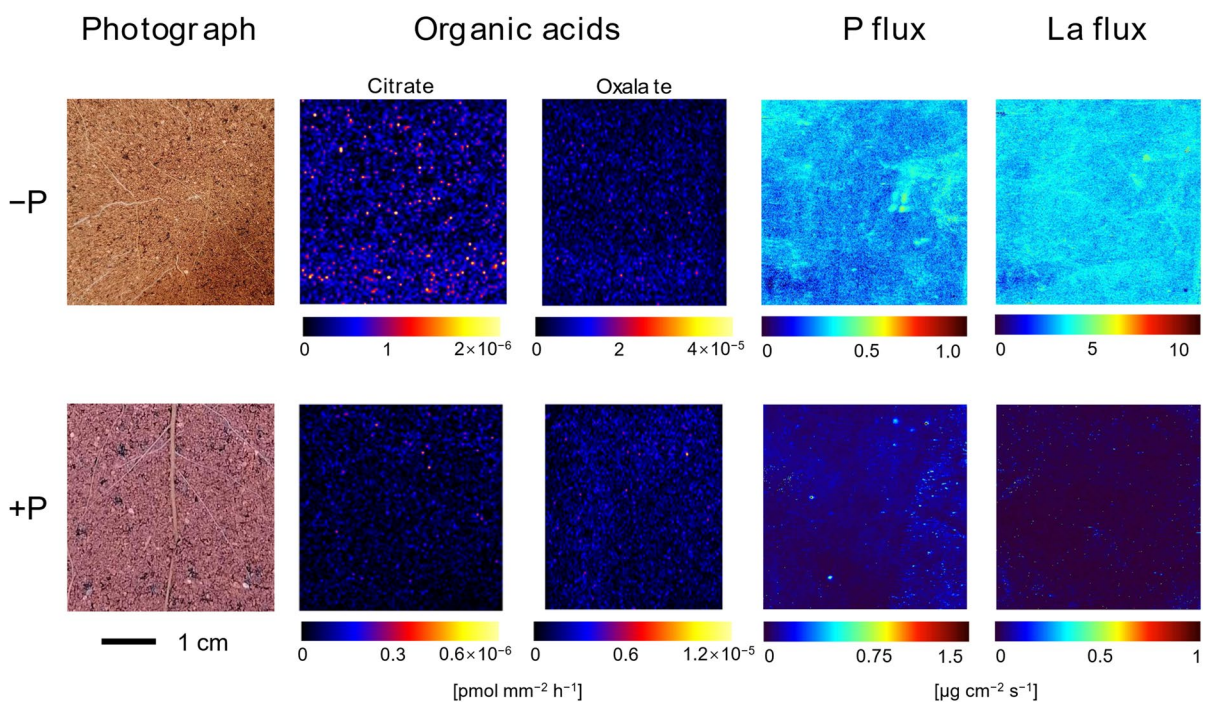


**Fig. 7** Spatial distribution of root exudates, phosphorus (P) and lanthanum (La) in the rhizosphere of *P. americana*. (Column 1) Images of *P. americana* rhizosphere and regions of interest; (Column 2–3) Spatial distribution of organic acids in the rhizosphere of *P. americana* detected by DESI-MS; (Columns 4–5) Spatial distribution of P and La in the rhizosphere of *P. americana* detected by LA-ICP-MS. -P, P deficient; +P, P sufficient conditions

therefore synchronously characterize the spatial distribution of multiple elements in the same rhizosphere hotspots. This novel approach can be used to study the distribution patterns of labile elements and root exudates at different plant growth stages. The surface of the DGT device used in this study is covered with a hydrophilic PVDF membrane, which acts as a filter for soil particles during the DGT sampling (Fig. 2). Thus, the binding and diffusion gels used for the elemental mapping are free from contamination from the soil. Moreover, due to the ability of PVDF membrane to adsorb organic acids (Figs. 5 and 6), we use the PVDF membrane as an adsorption carrier for root exudates. This achieves dual-purpose and synchronous quantitative measurement of the spatial distribution of elements and root exudates in the rhizosphere. Therefore, the combination of DGT and DESI imaging analysis will not affect each other.

However, it should be pointed out that the activity range of rhizosphere microorganisms almost overlaps with the root exudates, because root exudates provide important energy source for microbial growth (Kuzyakov and Razavi 2019). This means that root exudates may be degraded by microorganisms during the migration process towards the PVDF membrane and the root exudates adsorbed into the membrane may also been degraded. In this study, plant roots and soil showed clear separation on the detachable slide of rhizobox (Figs. 1b and 6). In addition, the PVDF membrane and root system are in close contact, and organic acids can be quickly absorbed by the membrane, while the smaller pore size of the membrane (0.45 μm) can isolate most microorganisms. Meanwhile, as Fig. 7 implies, the overall spatial distribution effect is still not satisfactory compared to Fig. 6. This may be related to the properties of organic acids and the soil moisture content in the rhizobox. DGT often requires a high soil moisture content (80%), which may promote the diffusion of organic acids at the root soil interface, resulting in a decrease of spatial resolution. In the future, optimizing plant growth medium parameters and

selecting the optimal conditions for the combination of the two can be considered. We believe that through adjustments in soil moisture and plant conditions, this method could simultaneously obtain high-resolution spatial distribution imaging of root exudates and labile elements.

### Mobilization of REEs and P in rhizosphere by root exudates of *P. americana*

Phosphorus deficiency induced root exudation plays an important role in plant P acquisition (Cesco et al. 2021; Lambers et al. 2015, 2021; Santner et al. 2012; Tiziani et al. 2020). This is because the secretion of organic acids (e.g., citrate) causes large amount of labile P from the P-containing minerals to be released. Combining DGT with LA-ICP-MS imaging, Kreuzeder et al. (2018) found that P accumulated around the root tip of white lupin. In the present study, PVDF-DGT sampling combined with DESI-MS and LA-ICP-MS mapping showed that P deficiency induced organic acid release causes the accumulation of plant-available P, REEs and nutrient elements in the rhizosphere soil of *P. americana* (Fig. 7, Fig. S1). This result thus provides visual evidence that organic acids released by *P. americana* in the rhizosphere play an important role in mobilizing P and REEs in the rhizosphere soil, leading to inadvertent uptake and accumulation of REEs in this species.

The distribution of root exudates based on PVDF-DESI-MS shows that, the oxalate flux in the rhizosphere of *P. americana* was 20 greater than citrate, and the oxalate flux under P deficiency was three times higher than in the P sufficient treatment (Fig. 7). This suggests that oxalate exudation is an important response of *P. americana* roots to counter P deficiency. In a previous study, we found that oxalate can effectively mobilize P, but will not release soil-bound REEs (Liu et al. 2023), which might explain how *P. americana* simultaneously copes with P deficiency and REE toxicity. However, a small amount of other organic acids (e.g., citrate and malate) can effectively mobilize REEs, thereby increasing REE flux and enrichment on the root surface (Fig. 7). Our recent study has also revealed that oxalate had limited contribution to REE exclusion by *P. americana* roots, while citrate and malate promote REE translocation from the roots to shoots (Liu et al. 2022).

## Conclusions

We developed a novel approach for in situ sampling and quantitative imaging of various parameters in the rhizosphere, achieving synchronous characterization of the spatial distribution of root exudates and nutrition and trace elements at sub-millimeter spatial resolution. This method combines DGT-LA-ICP-MS with PVDF-DESI-MS to overcome the limitations of existing methods in its operation complexity, single target analyte, matrix interferences, non-in situ and non-quantitative. In the new approach demonstrated here, we show that under P deficiency, organic acid secretion enhances enrichment of P and REEs in the rhizosphere, which is a key rhizosphere process for soil REE mobilization and subsequent REE hyperaccumulation in *P. americana*. In summary, this study presents a straightforward method to obtain the spatial distribution of labile elements and root exudates in rhizosphere hotspots. This method is applicable to laboratory (e.g., rhizobox) and as well as in the field (e.g., root window). The visualization at the root-soil interface is a powerful tool for better understanding of nutrient efficiency induced rhizosphere effects by plants. This approach presented here does have some limitations, including the limited spatial fidelity of the organic acids in the rhizosphere of *P. americana* due to partial diffusion effects. The optimization of soil parameters and analytical conditions and combining DESI, DGT with planar optode and zymography should be investigated further.

**Acknowledgments** We thank Ms. Hai-Yun Zhou (Instrumental Analysis & Research Center, Sun Yat-Sen University) for her help in DESI-MS analysis.

**Author contributions** Chong Liu: Conceptualization, Methodology, Investigation, Writing - Original Draft, Visualization. Ting-Xuan Ding: Methodology, Investigation, Visualization. Antony van der Ent, Chang Liu: Writing - Review & Editing. Wen-Shen Liu: Writing-Review & Editing, Funding acquisition. Jean Louis Morel, Catherine Sirguey: Review. Ye-Tao Tang, Rong-Liang Qiu: Supervision, Writing - Review & Editing, Funding acquisition.

**Funding** This work was supported by the National Natural Science Foundation of China (41771343, 41920104003, 41877475, 42007110) and the 111 Project (B18060).

**Data availability** The datasets generated during and/or analyzed during the current study are available from the corresponding author on reasonable request.

**Declarations**

**Competing interests** The authors have no relevant financial or non-financial interests to disclose.

## References

Álvarez-López V, Puschenreiter M, Santner J, Lehto N, Prieto-Fernández Á, Wenzel WW, Monterroso C, Kidd PS (2021) Evidence for nickel mobilisation in rhizosphere soils of Ni hyperaccumulator *Odontarrhena serpyllifolia*. Plant Soil 464:89–107

Badri DV, Vivanco JM (2009) Regulation and function of root exudates. Plant Cell Environ 32(6):666–681

Bhandari DR, Wang Q, Friedt W, Spengler B, Gottwald S, Römpp A (2015) High resolution mass spectrometry imaging of plant tissues: towards a plant metabolite atlas. Analyst 140(22):7696–7709

Cesco S, Lucini L, Miras-Moreno B, Borruso L, Mimmo T, Pii Y, Puglisi E, Spini G, Taskin E, Tiziani R, Zangrillo MS, Trevisan M (2021) The hidden effects of agrochemicals on plant metabolism and root-associated microorganisms. Plant Sci 311:111012

Chen YT, Wang Y, Yeh KC (2017) Role of root exudates in metal acquisition and tolerance. Curr Opin Plant Biol 39:66–72

Davison W, Zhang H (1994) In situ speciation measurements of trace components in natural waters using thin-film gels. Nature 367(6463):546–548

DeGroote KV, McCartha GL, Pollard AJ (2018) Interactions of the manganese hyperaccumulator *Phytolacca americana* L. with soil pH and phosphate. Ecol Res 33(4):749–755

Gomez-Zepeda D, Frausto M, Nájera-González H-R, Herrera-Estrella L, Ordaz-Ortiz J-J (2021) Mass spectrometry-based quantification and spatial localization of small organic acid exudates in plant roots under phosphorus deficiency and aluminum toxicity. Plant J 106(6):1791–1806

Gregory PJ, George TS, Paterson E (2022) New methods for new questions about rhizosphere/plant root interactions. Plant Soil 476:699–712

Guan D-X, He S-X, Li G, Teng HH, Ma LQ (2021) Application of diffusive gradients in thin-films technique for speciation, bioavailability, modeling and mapping of nutrients and contaminants in soils. Crit Rev Environ Sci Technol 52(7):3035–3079

Günther D, Hattendorf B (2005) Solid sample analysis using laser ablation inductively coupled plasma mass spectrometry. TrAC Trends Anal Chem 24(3):255–265

Han F, Shan X-Q, Zhang J, Xie Y-N, Pei Z-G, Zhang S-Z, Zhu Y-G, Wen B (2005) Organic acids promote the uptake of lanthanum by barley roots. New Phytol 165(2):481–492

Kreuzeder A, Santner J, Scharsching V, Oburger E, Hoefer C, Hann S, Wenzel WW (2018) In situ observation of localized, sub-mm scale changes of phosphorus biogeochemistry in the rhizosphere. Plant Soil 424(1):573–589

Kuzyakov Y, Razavi BS (2019) Rhizosphere size and shape: temporal dynamics and spatial stationarity. Soil Biol Biochem 135:343–360

Lambers H, Hayes PE, Laliberté E, Oliveira RS, Turner BL (2015) Leaf manganese accumulation and phosphorus-acquisition efficiency. Trends Plant Sci 20(2):83–90

Lambers H, Wright IJ, Guilherme Pereira C, Bellingham PJ, Bentley LP, Boonman A, Cernusak LA, Foulds W, Gleason SM, Gray EF, Hayes PE, Kooyman RM, Malhi Y, Richardson SJ, Shane MW, Staudinger C, Stock WD, Swarts ND, Turner BL, Turner J, Veneklaas EJ, Wasaki J, Westoby M, Xu Y (2021) Leaf manganese concentrations as a tool to assess belowground plant functioning in phosphorus-impoverished environments. Plant Soil 461:43–61

Lehto NJ, Davison W, Zhang H (2012) The use of ultra-thin diffusive gradients in thin-films (DGT) devices for the analysis of trace metal dynamics in soils and sediments: a measurement and modelling approach. Environ Chem 9(4):415–423

Liu W-S, Chen Y-Y, Huot H, Liu C, Guo M-N, Qiu R-L, Morel JL, Tang Y-T (2020) Phytoextraction of rare earth elements from ion-adsorption mine tailings by *Phytolacca americana*: Effects of organic material and biochar amendment. J Clean Prod 275:122959

Liu C, Ding T-X, Liu W-S, Tang Y-T, Qiu R-L (2023) Phosphorus mediated rhizosphere mobilization and apoplast precipitation regulate rare earth element accumulation in *Phytolacca americana*. Plant Soil 483:697–709

Liu C, Liu W-S, van der Ent A, Morel JL, Zheng H-X, Wang G-B, Tang Y-T, Qiu R-L (2021) Simultaneous hyperaccumulation of rare earth elements, manganese and aluminum in *Phytolacca americana* in response to soil properties. Chemosphere 282:131096

Liu C, Sun D, Zheng H-X, Wang G-B, Liu W-S, Cao Y, Tang Y-T, Qiu R-L (2022) The limited exclusion and efficient translocation mediated by organic acids contribute to rare earth element hyperaccumulation in *Phytolacca americana*. Sci Total Environ 805:150335

Monei N, Hitch M, Heim J, Pourret O, Heilmeier H, Wiche O (2022) Effect of substrate properties and phosphorus supply on facilitating the uptake of rare earth elements (REE) in mixed culture cropping systems of *Hordeum vulgare*, *Lupinus albus* and *Lupinus angustifolius*. Environ Sci Pollut Res 29:57172–57189

Oburger E, Jones DL (2018) Sampling root exudates – mission impossible? Rhizosphere 6:116–133

Oburger E, Schmidt H (2016) New methods to unravel rhizosphere processes. Trends Plant Sci 21(3):243–255

Pollard AJ (2022) Inadvertent uptake of trace elements and its role in the physiology and evolution of hyperaccumulators. Plant Soil 483:711–719

Pollard AJ, Reeves RD, Baker AJM (2014) Facultative hyperaccumulation of heavy metals and metalloids. Plant Sci 217–218:8–17

Ren M, Ding S, Dai Z, Wang J, Li C, Zhong Z, Cao J, Yang L, Tsang DCW, Xu S, Yang C, Wang Y (2021) A new DGT technique comprising a hybrid sensor for the simultaneous high resolution 2-D imaging of sulfides, metallic cations, oxyanions and dissolved oxygen. J Hazard Mater 403:123597

Santner J, Zhang H, Leitner D, Schnepf A, Prohaska T, Puschenreiter M, Wenzel WW (2012) High-resolution chemical imaging of labile phosphorus in the rhizosphere of *Brassica napus* L. cultivars. Environ Exp Bot 77:219–226

Singh S, Parihar P, Singh R, Singh VP, Prasad SM (2016) Heavy metal tolerance in plants: role of transcriptomics, proteomics, metabolomics, and ionomics. Front. Front Plant Sci 6:1143

Tao Q, Hou D, Yang X, Li T (2016) Oxalate secretion from the root apex of *Sedum alfredii* contributes to hyperaccumulation of Cd. Plant Soil 398(1–2):139–152

Tao Q, Zhao J, Li J, Liu Y, Luo J, Yuan S, Li B, Li Q, Xu Q, Yu X, Huang H, Li T, Wang C (2020) Unique root exudate tartaric acid enhanced cadmium mobilization and uptake in Cd-hyperaccumulator *Sedum alfredii*. J Hazard Mater 383:121177

Tiziani R, Mimmo T, Valentinuzzi F, Pii Y, Celletti S, Cesco S (2020) Root handling affects carboxylates exudation and phosphate uptake of white lupin roots. Front Plant Sci 11:584568

Tiziani R, Miras-Moreno B, Malacrinò A, Vescio R, Lucini L, Mimmo T, Cesco S, Sorgonà A (2022) Drought, heat, and their combination impact the root exudation patterns and rhizosphere microbiome in maize roots. Environ Exp Bot 203:105071

Tiziani R, Puschenreiter M, Smolders E, Mimmo T, Herrera JC, Cesco S, Santner J (2021) Millimeter-resolution mapping of citrate exuded from soil grown roots using a novel, low-invasive sampling technique. J Exp Bot 72(10):3513–3525

van der Ent A, Baker AJM, Reeves RD, Pollard AJ, Schat H (2013) Hyperaccumulators of metal and metalloid trace elements: facts and fiction. Plant Soil 362(1):319–334

van der Ent A, Nkrumah PN, Purwadi I, Erskine PD (2022) Rare earth element (hyper)accumulation in some Proteaceae from Queensland, Australia. Plant Soil 485:247–257

Veličković D, Anderton CR (2017) Mass spectrometry imaging: towards mapping the elemental and molecular composition of the rhizosphere. Rhizosphere 3:254–258

Veličković D, Lin VS, Rivas A, Anderton CR, Moran JJ (2020) An approach for broad molecular imaging of the root-soil interface via indirect matrix-assisted laser desorption/ionization mass spectrometry. Soil Biol Biochem 146:107804

White RA, Rivas-Ubach A, Borkum MI, Köberl M, Bilbao A, Colby SM, Hoyt DW, Bingol K, Kim Y-M, Wendler JP, Hixson KK, Jansson C (2017) The state of rhizospheric science in the era of multi-omics: a practical guide to omics technologies. Rhizosphere 3:212–221

Wiche O, Kummer N-A, Heilmeier H (2016) Interspecific root interactions between white lupin and barley enhance the uptake of rare earth elements (REEs) and nutrients in shoots of barley. Plant Soil 402(1):235–245

Williams PN, Santner J, Larsen M, Lehto NJ, Oburger E, Wenzel W, Glud RN, Davison W, Zhang H (2014) Localized flux maxima of arsenic, lead, and iron around root apices in flooded lowland rice. Environ Sci Technol 48(15):8498–8506

Yang X, Qin J, Li J, Lai Z, Li H (2021) Upland rice intercropping with *Solanum nigrum* inoculated with arbuscular mycorrhizal fungi reduces grain cd while promoting phytoremediation of Cd-contaminated soil. J Hazard Mater 406:124325